PHYSICAL REVIEW B **82**, 060513(R) (2010)

Ultrafast charge dynamics in photoexcited Nd_2CuO_4 and La_2CuO_4 cuprate compounds investigated by femtosecond absorption spectroscopy

H. Okamoto,[1,2,3] T. Miyagoe,[1] K. Kobayashi,[1] H. Uemura,[1] H. Nishioka,[1] H. Matsuzaki,[1] A. Sawa,[2,3] and Y. Tokura[3,4]
[1]*Department of Advanced Materials Science, University of Tokyo, Chiba 277-8561, Japan*
[2]*CREST, Japan Science and Technology Agency, Chiyoda-ku, Tokyo 102-0075, Japan*
[3]*National Institute of Advanced Industrial Science and Technology (AIST), Tsukuba 305-8562, Japan*
[4]*Department of Applied Physics, University of Tokyo, Tokyo 113-8656, Japan*
(Received 25 June 2010; published 24 August 2010)

Charge and lattice dynamics caused by photocarrier doping of the undoped cuprates Nd_2CuO_4 and La_2CuO_4 were studied by femtosecond absorption spectroscopy. In both compounds, a metallic state is formed just after photoexcitation and decays within ~200 fs. Photogenerated electrons and holes are subsequently localized due to charge-spin coupling, producing midgap absorptions at different energies. Charge-phonon coupling also occurs in both compounds. This is more significant for La_2CuO_4 than for Nd_2CuO_4, and leads to higher midgap absorption energies, and slower recombination of polaronic carriers. The role of apical oxygen atoms in charge-phonon coupling in La_2CuO_4 is also discussed.

DOI: 10.1103/PhysRevB.82.060513 PACS number(s): 71.38.−k, 74.72.−h, 78.47.−p

The study of charge dynamics in cuprates is important in forming an understanding of the insulator-metal transitions and high-T_c superconductivity induced by carrier doping of CuO_2 layers. In underdoped cuprates, such as electron-doped Nd_2CuO_4 ($Nd_{2-x}Ce_xCuO_4$) and hole-doped La_2CuO_4 ($La_{2-x}Sr_xCuO_4$), electrons and holes cannot move freely in the antiferromagnetic (AF) spin background because of the coupling of charge and spin degrees of freedom, resulting in midgap absorptions (incoherent parts).[1–3] Further carrier doping gives rise to metallic states but the Drude weight (coherent part) is small compared to the incoherent part.[2,3] The importance of charge-phonon (CP) coupling for doped holes has also been suggested by angle-resolved photoelectron spectra[4–7] and optical conductivity spectra.[8] Both charge-spin (CS) and CP coupling are therefore important aspects of hole dynamics. CP coupling may also play an essential role in the behavior of doped electrons although little information on electron dynamics has been reported to date. Clarifying the role of CP coupling in the behavior of doped electrons, as well as in the behavior of doped holes, is probably important in understanding superconductivity pairing mechanisms,[9] since there is still controversy over whether or not CP coupling is essential.

In this study, we performed femtosecond (fs) pump-probe (PP) absorption spectroscopy from the visible to the infrared (IR) region on typical cuprate parent compounds, Nd_2CuO_4 (NCO) and La_2CuO_4 (LCO). As shown in Figs. 1(a) and 1(b), each CuO plane consists of CuO_6 octahedrons in LCO (Ref. 10) but there are no apical oxygen atoms in NCO.[11] In both compounds, a metallic state is formed just after photoexcitation and decays very rapidly, within ~200 fs. Electrons and holes are subsequently localized as a result of CS coupling, producing midgap absorptions at different energies. In LCO, we observed different behaviors from those observed in NCO, namely, higher energy shifts of the midgap absorptions and relatively slow decay of photocarriers. These features are discussed in terms of larger CP coupling in LCO.

Epitaxial thin films of NCO and LCO were grown by pulsed laser deposition on the nearly lattice-matched substrates $(LaAlO_3)_{0.3}(SrAl_{0.5}Ta_{0.5}O_3)_{0.7}$ and $LaSrAlO_4$ (LSAO), respectively, with the CuO planes parallel to the substrates.[12] As reference materials, we prepared 1% electron-doped NCO, $Nd_{1.99}Ce_{0.01}CuO_4$ (NCCO), and 2% hole-doped LCO, $La_{1.98}Sr_{0.02}CuO_4$ (LSCO). The thickness of the films was 120 nm for NCO and NCCO, and 100 nm for LCO and LSCO. For the PP measurements, we used a $Ti:Al_2O_3$ regenerative amplifier as a light source (photon energy 1.55 eV, pulse width 130 fs, and repetition rate 1 kHz). The output from the amplifier was divided into two beams, which were used as excitation sources for two optical parametric amplifiers (OPAs). From these two OPAs, pump (1.58 and 2.25 eV) and probe (0.1–2.2 eV) pulses were obtained. The delay time t_d of the probe pulse relative to the pump pulse was controlled by changing the path length of the pump pulse. The time resolution of the system was ~200 fs. The excitation photon density x_{ph} was evaluated from $x_{ph}=I_p(1-R_p)(1-1/e)/l_p$, where, I_p, l_p, and R_p are the excitation photon density per unit area, the absorption depth, and the reflection loss of the pump light, respectively. The beams had Gaussian profiles and the beam diameters were 500 μm for the pump beam and 150 μm for the probe

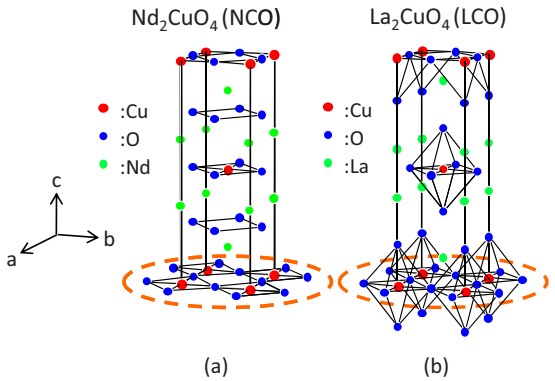

FIG. 1. (Color online) Crystal structures of (a) NCO and (b) LCO.

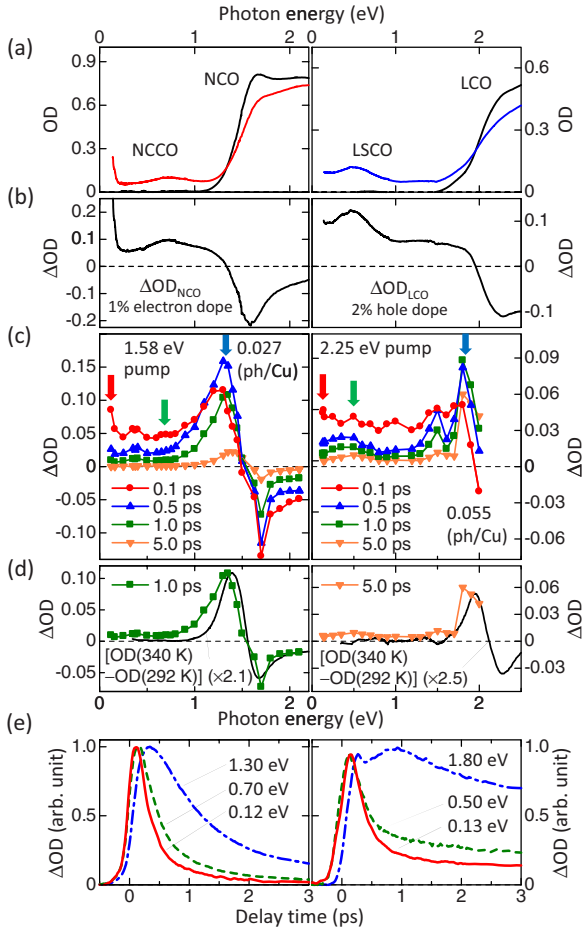

FIG. 2. (Color online) (a) OD spectra of NCO, NCCO, LCO, and LSCO. (b) The differential OD spectra ΔOD_{NCO} (ΔOD_{LCO}) of NCO (LCO) and NCCO (LSCO). (c) Photoinduced absorption (ΔOD) spectra with pump energy of 1.58 eV (NCO) and 2.25 eV (LCO). (d) ΔOD spectra at 1 ps of NCO and 5 ps of LCO. Solid lines show the differential OD spectra [OD(340 K)–OD(292 K)]. (e) Time characteristics of ΔOD at the energies indicated by arrows in (c).

beam. All measurements were performed at room temperature (292 K).

Absorption (OD: optical density) spectra of NCO and LCO are shown in Fig. 2(a). The shoulder structures at 1.65 eV for NCO and 2.2 eV for LCO are attributable to the charge-transfer (CT) transition from the occupied oxygen $2p$ band to the copper $3d$ upper Hubbard band. In the same figure, we also show OD spectra of NCCO and LSCO, in which midgap absorptions appear at around 0.7 eV in NCCO and 0.5 eV in LSCO. In NCCO, the OD spectrum shows a sharp increase below 0.2 eV, attributable to a Drude-type metallic response. In LSCO, such a clear increase in the OD could not be observed because of the limitations of the transparent region of the substrate (LSAO). However, the onset of an increase in OD was seen at 0.12 eV. In Fig. 2(b), we show the differential absorption spectrum, ΔOD_{NCO} (ΔOD_{LCO}), of NCCO (LSCO) and NCO (LCO), which corresponds to the absorption change due to the 1% electron (2% hole) doping in NCO (LCO).

The spectra of the photoinduced absorption changes ΔOD resulting from excitation of the CT gap transition (1.58 eV for NCO and 2.25 eV for LCO) are shown in Fig. 2(c) for several t_d values.[13] The excitation photon densities x_{ph} are 0.027 photons/Cu in NCO and 0.055 photons/Cu in LCO. First, we discuss the spectral features of ΔOD by dividing them into three regions: the IR region for $\hbar\omega < 0.2$ eV, the near-IR (NIR) region for $\hbar\omega > 1.0$ eV in NCO and for $\hbar\omega > 1.5$ eV in LCO, and the residual mid-IR (MIR) region. For the MIR to IR region, we show in Fig. 3 expanded ΔOD spectra with a normalized scale to enable the spectral changes with time to be seen more clearly.

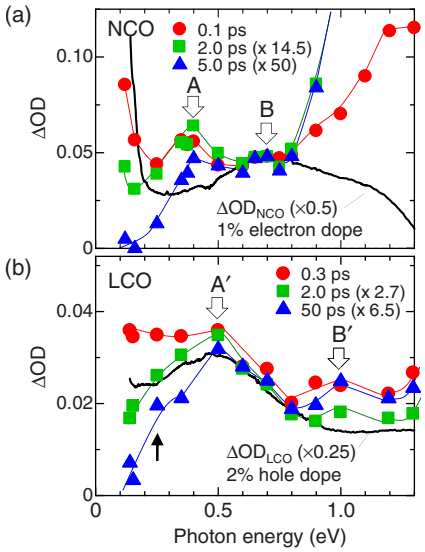

FIG. 3. (Color online) Expanded ΔOD spectra with a normalized scale in (a) NCO and (b) LCO. Solid lines show ΔOD_{NCO} and ΔOD_{LCO}.

In the IR region, ΔOD at $t_d = 0.1$ ps increases monotonically with decreasing energy for both compounds, showing Drude-type behavior [Figs. 2(c) and 3]; that is, the metallic states are photogenerated. In the MIR region, a broad midgap absorption is observed. These Drude-type components and midgap absorptions resemble the absorption changes ΔOD_{NCO} in NCCO and ΔOD_{LCO} in LSCO caused by chemical carrier doping [Fig. 2(b)]. As seen in Fig. 3(a), in NCO, the Drude-type component below 0.2 eV decreases more rapidly than the midgap absorption. In LCO, the ΔOD spectra show a similar tendency.

In the ΔOD spectra of the NIR region, peak structures appear at around 1.3 eV in NCO and 1.8 eV in LCO; these peaks are not present in NCCO and LSCO. In Fig. 2(d), we show the ΔOD spectra at 1 ps for NCO and at 5 ps for LCO, in which the peak structures in the NIR region are more distinct than the midgap absorptions. Their spectral shapes are in good agreement with the spectral changes [OD(340 K)–OD(292 K)] induced by an increase in temperature from 292 to 340 K [solid lines in Fig. 2(d)]. Therefore, the NIR ΔOD peaks can be attributed to a heating effect, which occurs by rapid photocarrier recombinations and thermalizations of electron, spin, and lattice systems. The photoinduced absorption increase in the NIR region was previously reported in NCO (Ref. 14) and has recently been reported in $Sr_2CuO_2Cl_2$.[15] In the latter, the similar explanation is also possible.[15]

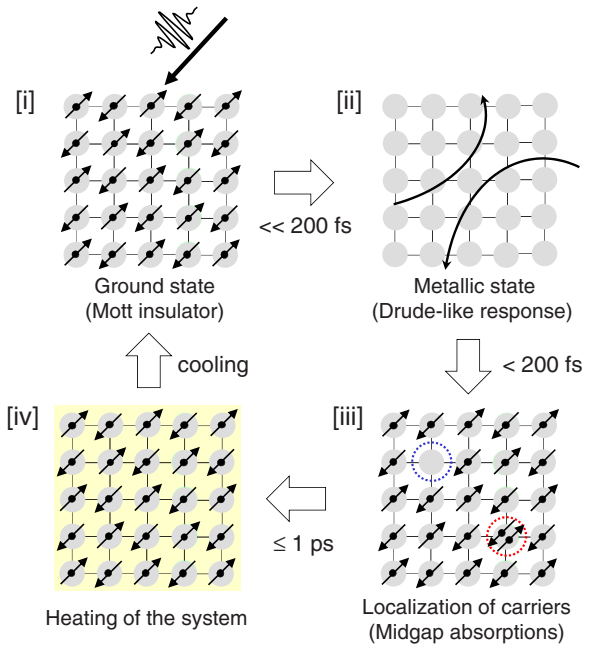

FIG. 4. (Color online) Schematic view of photoinduced phenomena in NCO: (i) ground state of the Mott insulator, (ii) photoinduced metallic states showing the Drude response, (iii) localized carriers showing the mid-gap absorption, and (iv) heating of the system after photocarrier recombinations.

Figure 2(e) shows the time characteristics of ΔOD at 0.12 eV (0.13 eV), 0.70 eV (0.50 eV), and 1.30 eV (1.80 eV) in NCO (LCO), which reflect metallic states, midgap absorptions, and heating effects, respectively. In both compounds, the primary response in the IR region is very fast, indicating that the initial decay of the metallic state occurs within a time resolution of 200 fs. In NCO, the midgap absorption also decays rapidly, within ~1 ps or less. In LCO, the decay of the midgap absorption for $t_d > 0.3$ ps takes much longer; however, it decays completely within 500 ps (not shown). Long-lived ΔOD signals, which are observed in steady-state measurements on the powder samples at low temperatures,[16] never exist. The ΔOD signals in the NIR region resulting from heating effects appear after a delay and have long decay times corresponding to the cooling process. The overall dynamics in NCO are illustrated schematically in Fig. 4.

Next, we discuss the nature of the midgap absorptions in more detail by scrutinizing the ΔOD spectra in Fig. 3. In both compounds, two midgap absorption peaks, **A** at 0.4 eV and **B** at ~0.7 eV in NCO, and **A′** at 0.5 eV and **B′** at ~1.0 eV in LCO, are observed. In Fig. 3, we also plotted the ΔOD_{NCO} spectrum resulting from chemical electron doping in NCO, and the ΔOD_{LCO} spectrum resulting from chemical hole doping in LCO. Peak **B** in NCO corresponds well to the peak in ΔOD_{NCO}, indicating that peak **B** is caused by electron carriers. Peak **A′** in LCO corresponds well to the peak in ΔOD_{LCO}, indicating that peak **A′** is caused by hole carriers. Photoirradiation generates an electron-hole pair. Consequently, peak **A** in NCO and **B′** in LCO can reasonably be attributed to hole carriers and electron carriers, respectively.

In the ΔOD spectra at 5 ps for NCO and 50 ps for LCO (triangles in Fig. 3), the low-energy spectral weight in the IR region disappears and the midgap absorptions caused by localized carriers are clearly observed. From a comparison of the magnitude of ΔOD with those of ΔOD_{NCO} or ΔOD_{LCO}, the electron and hole densities were evaluated as 1×10^{-4}/Cu at 5 ps in NCO and 8×10^{-4}/Cu at 50 ps in LCO, respectively. The carrier densities are very small, so ΔOD at 5 ps in NCO and at 50 ps in LCO can be considered to represent the spectra of isolated single-electron and single-hole states.

We can now compare our midgap absorption spectra with the doping-induced absorption changes predicted by theoretical studies.[17–20] According to the *t-J* model, including long-range hopping *t′* and *t″*, which is called the *t-t′-t″-J* model, the AF spin configuration in a single-electron state is more stable than that in a single-hole state.[20] This results in a higher absorption energy for a single-electron state than for a single-hole state. This explains well the energy difference between **A** and **B** in NCO, and between **A′** and **B′** in LCO. An important observation is that the energies of **A′** and **B′** in LCO are relatively large compared to the energies of **A** and **B** in NCO. In particular, the blueshift of **B′** is very large (~0.3 eV).

Taking the CS coupling into account, the peak structures of the midgap absorptions can be considered to be magnon side bands and their energies are scaled by the AF exchange interaction *J*.[8] According to neutron-scattering studies, the *J* value of NCO is 155 meV, which is nearly the same as the *J* value of LCO (133 meV).[21] Thus, the higher peak energies of **A′** and **B′** in LCO cannot be explained by CS coupling. A possible origin for the higher peak energies is CP coupling. According to recent theoretical calculations based on the *t-J* model, the introduction of CP coupling gives rise to drastic changes in the optical conductivity spectra in single-hole states because of polaron formation;[8] with an increase in CP coupling, the main peak due to the magnon side band shifts to higher energy, and the shoulder structure due to the phonon side band on the lower energy side increases in intensity. It is reasonable to suppose that the former is responsible for the blue shift of peak **A′** and that the CP coupling is larger in LCO than in NCO. The blue shift of peak **B′** would have a similar origin. The larger shift of peak **B′** suggests that CP coupling is more significant in an electron state than in a hole state. A more careful comparison of the spectral shapes of ΔOD in NCO and in LCO indicates the presence of a shoulder structure below peak **A′** only in LCO [the arrow in Fig. 3(b)]. This may be assigned to the phonon side band. When carriers are localized as polarons, their decay time is dominated by the encounter rate of electrons and hole polarons. The larger CP coupling in LCO suppresses polaron mobility and therefore increases their decay time compared to those in NCO.

Here, we discuss the origin of the difference between CP coupling in NCO and in LCO. An important difference is that apical oxygen atoms exist in LCO but not in NCO. Previous studies revealed that the removal of apical oxygen atoms decreases the gap energy and destabilizes doped holes.[22] In NCO, the gap energy is smaller and chemical hole doping is very difficult. The *J* values[21] indicate that the effective *pd* hybridization in NCO is not very different from that in LCO, in spite of the smaller gap energy. This is because in NCO

the longer Cu-O distance cancels out the enhancement of the effective *pd* hybridization resulting from the smaller gap energy. Thus the difference in the effects of CP coupling cannot be attributed to the difference in gap energies. Moreover, the correlation between the stability of a doped hole and the presence of apical oxygen atoms cannot be directly related to the magnitude of the CP coupling. The apical oxygen atom effect to be considered is their direct contribution to CP coupling. A theoretical study suggested that the CP coupling in a doped hole due to the apical-oxygen mode is not negligible compared with that due to the planar-oxygen mode.[7] Therefore, the stronger CP coupling in a doped hole in LCO, compared with that in NCO, is attributable to apical oxygen atoms. The larger blue shift (~0.3 eV) of the electron peak **B′** in LCO from the peak **B** in NCO compared to that (~0.1 eV) of the hole peak **A′** from the peak **A**, suggests that a doped electron is stabilized more strongly than a doped hole by displacements of apical oxygen atoms. The site-diagonal-type CP coupling caused by apical oxygen atoms would play a dominant role in electron stabilization since it has Cu *d* characteristics. To clarify this point, theoretical studies based on the two-band model would be necessary since the electron-hole asymmetry caused by CP coupling cannot be addressed in the *t-J* model.

It is useful to discuss the magnitudes of the CP coupling in the two compounds quantitatively. For this purpose, we compare peaks **A** and **A′** to the theoretical doped-hole absorption peaks calculated for various magnitudes of the CP-coupling constant λ.[8] Since the values of *J* in NCO and LCO are roughly the same, we can deduce the relative magnitudes of λ from the energy positions of peaks **A** (0.4 eV) and **A′** (0.5 eV). Using these values, and the relation between the peak energies of the midgap absorption and λ shown in Fig. 4(a) of Ref. 8, the value of λ in NCO is estimated to be ~80% that of λ in LCO. The larger value of λ in LCO can be related to the apical oxygen atoms but this estimate is only valid for a single-hole carrier, as discussed above.

In summary, fs pulse excitation in Nd_2CuO_4 and La_2CuO_4 generates a metallic state, which rapidly decays. The photocarriers are subsequently localized, producing two midgap absorptions due to electrons and holes. Charge-phonon coupling is more significant in La_2CuO_4 than in Nd_2CuO_4, probably because of the presence of apical oxygen atoms. This is responsible for the higher midgap absorption energies and the slower recombination of polaronic carriers in La_2CuO_4. The results demonstrate the importance of charge-phonon coupling for both electron and hole carriers. Such information will lead to an increased understanding of the electronic properties in underdoped cuprates, and possibly to the mechanism of high-T_c superconductivity.

The authors wish to thank N. Nagaosa, A. S. Mishchenko, T. Tohyama, S. Ishihara, and A. Fujimori for enlightening discussions. This work was supported in part by MEXT (Grants No. 16076207 and No. 20110005).

[1] S. L. Cooper, G. A. Thomas, J. Orenstein, D. H. Rapkine, A. J. Millis, S-W. Cheong, A. S. Cooper, and Z. Fisk, Phys. Rev. B **41**, 11605 (1990).

[2] S. Uchida, T. Ido, H. Takagi, T. Arima, Y. Tokura, and S. Tajima, Phys. Rev. B **43**, 7942 (1991).

[3] Y. Onose, Y. Taguchi, K. Ishizaka, and Y. Tokura, Phys. Rev. B **69**, 024504 (2004).

[4] A. Lanzara, P. V. Bogdanov, X. J. Zhou, S. A. Kellar, D. L. Feng, E. D. Lu, T. Yoshida, H. Eisaki, A. Fujimori, K. Kishio, J.-I. Shimoyama, T. Noda, S. Uchida, Z. Hussain, and Z.-X. Shen, Nature (London) **412**, 510 (2001).

[5] K. M. Shen, F. Ronning, D. H. Lu, W. S. Lee, N. J. C. Ingle, W. Meevasana, F. Baumberger, A. Damascelli, N. P. Armitage, L. L. Miller, Y. Kohsaka, M. Azuma, M. Takano, H. Takagi, and Z.-X. Shen, Phys. Rev. Lett. **93**, 267002 (2004).

[6] X. J. Zhou, J. Shi, T. Yoshida, T. Cuk, W. L. Yang, V. Brouet, J. Nakamura, N. Mannella, S. Komiya, Y. Ando, F. Zhou, W. X. Ti, J. W. Xiong, Z. X. Zhao, T. Sasagawa, T. Kakeshita, H. Eisaki, S. Uchida, A. Fujimori, Z. Zhang, E. W. Plummer, R. B. Laughlin, Z. Hussain, and Z.-X. Shen, Phys. Rev. Lett. **95**, 117001 (2005).

[7] O. Rösch, O. Gunnarsson, X. J. Zhou, T. Yoshida, T. Sasagawa, A. Fujimori, Z. Hussain, Z.-X. Shen, and S. Uchida, Phys. Rev. Lett. **95**, 227002 (2005).

[8] A. S. Mishchenko, N. Nagaosa, Z.-X. Shen, G. De Filippis, V. Cataudella, T. P. Devereaux, C. Bernhard, K. W. Kim, and J. Zaanen, Phys. Rev. Lett. **100**, 166401 (2008).

[9] S. Ishihara and N. Nagaosa, Phys. Rev. B **69**, 144520 (2004).

[10] J. M. Longo and P. M. Raccah, J. Solid State Chem. **6**, 526 (1973).

[11] Y. Tokura, H. Takagi, and S. Uchida, Nature (London) **337**, 345 (1989).

[12] A. Sawa, M. Kawasaki, H. Takagi, and Y. Tokura, Phys. Rev. B **66**, 014531 (2002).

[13] There are errors of ~5% in ΔOD spectra at t_d=0.1 ps due to slight variations in temporal widths of probe pulses depending on photon energy. For t_d>0.2 ps, magnitudes of errors are smaller than 5% (i.e., smaller than the dot size).

[14] K. Matsuda, I. Hirabayashi, K. Kawamoto, T. Nabatame, T. Tokizaki, and A. Nakamura, Phys. Rev. B **50**, 4097 (1994).

[15] J. Dodge, A. Schumacher, L. Miller, and D. Chemla, arXiv:0910.5048 (unpublished).

[16] Y. H. Kim, A. J. Heeger, L. Acedo, G. Stucky, and F. Wudl, Phys. Rev. B **36**, 7252 (1987); J. M. Ginder, M. G. Roe, Y. Song, R. P. McCall, J. R. Gaines, E. Ehrenfreund, and A. J. Epstein, *ibid.* **37**, 7506 (1988); Y. H. Kim, S.-W. Cheong, and Z. Fisk, Phys. Rev. Lett. **67**, 2227 (1991).

[17] T. M. Rice and F. C. Zhang, Phys. Rev. B **39**, 815 (1989).

[18] W. Stephan and P. Horsch, Phys. Rev. B **42**, 8736 (1990).

[19] E. Dagotto, A. Moreo, F. Ortolani, D. Poilblanc, and J. Riera, Phys. Rev. B **45**, 10741 (1992).

[20] T. Tohyama and S. Maekawa, Phys. Rev. B **64**, 212505 (2001).

[21] P. Bourges, H. Casalta, A. S. Ivanov, and D. Petitgrand, Phys. Rev. Lett. **79**, 4906 (1997).

[22] Y. Ohta, T. Tohyama, and S. Maekawa, Phys. Rev. B **43**, 2968 (1991).